[3] C T. Tai, *Dyadic Green's Functions in Electromagnetic Theory*. Scranton, PA: Intext, 1971.
[4] L B. Felsen and N. Marcuvitz, *Radiation and Scattering of Waves* Englewood Cliffs, NJ: Prentice Hall, 1973
[5] Y Rahmat-Samii, "On the question of computation of the dyadic Green's function at the source region in waveguides and cavities," *IEEE Trans. Microwave Theory Tech*, vol. MTT-23, pp 762–765, Sept 1975.
[6] C. T Tai and P. Rozenfeld, "Different representations of dyadic Green's functions for a rectangular cavity," *IEEE Trans Microwave Theory Tech*, vol. MTT-24, pp. 597–601, Sept. 1976.
[7] M. Kisliuk, "The dyadic Green's functions for cylindrical waveguides and cavities," *IEEE Trans. Microwave Theory Tech.*, vol. MTT-28, pp 894–898, Aug. 1980.
[8] C T. Tai, "Dyadic Green's functions for a coaxial line," *IEEE Trans Antennas Propagat.*, vol. AP-31, no. 2, pp 355–358, Mar. 1983.
[9] A Q. Howard and D. B. Seidel, "Singularity extraction in kernel functions in closed region problems," *Radio Sci.*, vol 13, no. 3, pp. 425–429, May–June 1978.
[10] V. Daniele and M. Orefice, "Dyadic green's functions in bounded media," *IEEE Trans. Antennas Propagat.*, vol. AP-32, pp 193–196, Feb 1984.
[11] V Daniele, "New expressions of dyadic Green's functions in uniform waveguides with perfectly conducting walls," *IEEE Trans. Antennas Propagat.*, vol. AP-30, pp 497–499, May 1982.
[12] M Bressan and G Conciauro, "Rapidly converging expressions for dyadic Green's functions in two-dimensional resonators of circular and rectangular cross-section," *Alta Frequenza*, vol. LII, no. 3, pp 188–190, May–June 1983.
[13] M Bressan and G. Conciauro, "Rapidly converging expressions of electric dyadic Green's functions for resonators," in *Proc. 1983 URSI Symp on Electromagnetic Theory* (Santiago de Compostela, Spain), Aug. 23–26, 1983, pp. 41–44.
[14] M. Bressan, G. Conciauro, and C. Zuffada, "Waveguide modes via an integral equation leading to a real matrix eigenvalue problem," *IEEE Trans. Microwave Theory, Tech.*, pp. 1495–1504, Nov. 1984.

Characteristic Impedance Design Considerations for a High-Speed Superconducting Packaging System

JIRO TEMMYO AND HARUO YOSHIKIYO

Abstract —**The characteristic impedance influences of superconducting packaging systems (in particular, Josephson packaging) on the degradation in transmitted signal rise time, amplitude distortions and crosstalk, signal propagation delay, and amplitude decay at the inductive and resistive connectors with matched capacitors are quantitatively evaluated by using the ASTAP computer simulation. The present choice of the characteristic impedance $Z_0 = 10$–$12\ \Omega$ for a superconducting stripline is inadequate. Higher impedances of $Z_0 = 40$–$50\ \Omega$ are useful from the standpoint of noise performance improvement. At the same time, a higher impedance choice can make the ground connector numbers of each connector decrease, which is preferable for a large-scale packaging system.**

I. Introduction

In order to realize high-performance computing systems utilizing high-speed devices, such as Josephson junction devices and other high-speed semiconductor devices, it is necessary to use high-density packaging systems with small wiring delays. The electrical problems in the packaging system are decreasing the noise signals such as crosstalk and reflection at the various connectors, and minimizing the packaging delay. A three-dimensional superconducting packaging system consisting of superconducting striplines [1] and small connectors is useful for high-density packaging because lossless superconducting lines have few heating problems [2].

Manuscript received July 27, 1984; revised January 4, 1985.

The authors are with Atsugi Electrical Communication Laboratory, Nippon Telegraph and Telephone Public Corporation, 1839 Ono, Atsugi-shi, Kanagawa 243-01, Japan.

A matched-signal propagation system with superconducting striplines has excellent features such as a broad transmission frequency band and almost lossless characteristics. Conversely, signal distortion problems occur compared with other lossy packaging systems because the reflected signals and crosstalk do not decrease [3]–[6]. Added delays due to a matched capacitor at the inductive connectors, crosstalk between signal lines, and signal decay at the resistive connectors decrease the system operating margin.

On the other hand, electrical design considerations of a high-speed semiconductor computer package have been carried out by E. E. Davidson from the standpoint of system noise tolerance performance [7]. However, noise performance of the superconducting packaging system from the standpoint of the characteristic impedance influences on the system has not been determined.

The purpose of this paper is to clarify the optimum characteristic impedance design method for superconducting packaging systems, particularly the Josephson packaging system. The characteristic impedance influences of superconducting packaging systems on the noise performance, such as reflection and crosstalk etc., which are caused by the inductive connectors, was clarified by using the ASTAP [8] computer simulation. From the relationships between the characteristic impedance Z_0 and noise, delay performances are clarified as design charts. It is proposed that present choices of $Z_0 = 10$–$12\ \Omega$ are not adequate and higher values of Z_0 are superior from the standpoint of low noise and small delay performances of the system using a high-output superconducting driver and highly sensitive receiver circuits.

II. Circuit Simulation

A schematic and electrical diagram of the chip-to-chip signal path is shown in Fig. 1, where L_c^C is the chip-to-card bonding [9], [10] inductance, L_c^F is the fillet [11] inductance, L_c^{MC} is the microconnector [12] inductance, and R_c^C, R_c^F, and R_c^{MC} are the interconnection resistance at the chip bonding, fillet, and microconnector, respectively. Except for the mutual inductance of M_c^C at the chip bonding, other connector mutual inductances of M_c^F and M_c^{MC} are omitted for simplicity. Z_0 is the superconducting transmission-line impedance of the chip and the package. In a small Josephson system experiment [13], the rise time of the driver's output signal was increased to about 100 ps by an LC filter to reduce crosstalk and minimize the reflections from the inductive discontinuities of the microconnectors. Here, in order to reduce absolute values of self- and mutual-inductances, the ratio of signal connectors to ground connectors was 1 for both pins and fillets. However, the increase of that ratio is important and necessary, particularly when the packaging system becomes larger.

The signal reflection and crosstalk at the inductive connectors are determined by the absolute value of the inductances and the characteristic impedance Z_0, as shown in Fig. 2. Time-domain responses for the circuit of Fig. 1 are shown for the cases of $Z_0 = 10\ \Omega$ and $20\ \Omega$, using the ASTAP computer simulation. The current traces of Nos. 1–6 show the current waveforms at the portion Nos. 1–6 in Fig. 1 and the degradation of the transmitted high-speed signal. Here, it is assumed that the Josephson driver is approximated as a ramped input voltage positive going source. The entire lossless superconducting stripline length at chips, cards, fillets, and cards is a constant 4 mm, i.e., the propagation

0018-9480/85/0500-0414$01.00

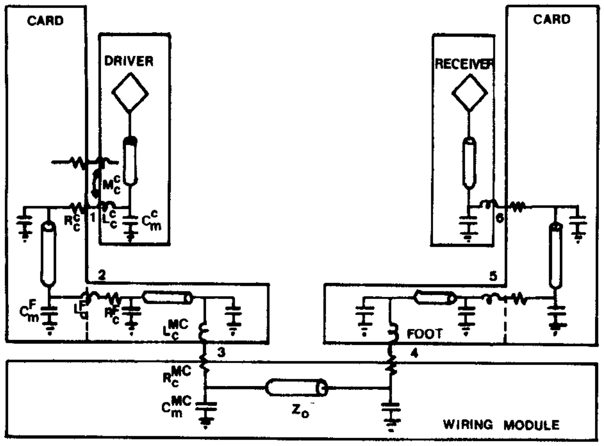

Fig. 1. An equivalent diagram of a chip-to-chip signal path in the superconducting package. The characteristic impedance of the transmission line on the package and chip is Z_0, constant.

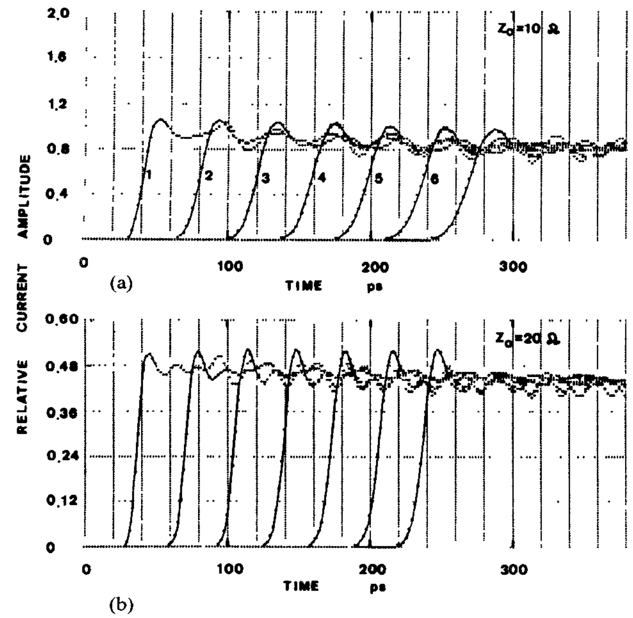

Fig. 2. Current waveforms for the matched circuit shown in Fig. 1, where L_c is 100 pH and $R_c = 0.5\ \Omega$. (a) $Z_0 = 10\ \Omega$. (b) $Z_0 = 20\ \Omega$.

delay is 30 ps, the lumped inductance values L_c, M_c are constants 100 pH and zero for simplicity, and interconnection resistance value R_c is a constant of 0.5 Ω. Matching capacitor values C_m are determined by the following equation:

$$C_m = \frac{L_c}{2Z_0^2} \tag{1}$$

where the upper suffixes C, F, and MC are omitted. The transmission line is terminated by the matched resistor $R_L = Z_0$. The degradation of the signal rise time, delay, reflection, and amplitude decay are intensively influenced by the characteristic impedance values, as shown in Fig. 2.

First, consider the electrical noise properties of the circuit for the characteristic impedance Z_0. The degradation of the rise time t_r of the transmitted signal is shown in Fig. 3. The relationship between the signal rise time and the summed inductive value after passing through some connectors with and/or without matching capacitors is shown. As a characteristic impedance value becomes larger, the rise-time degradation abruptly becomes smaller, which is somewhat improved by the matched capacitors. The difference

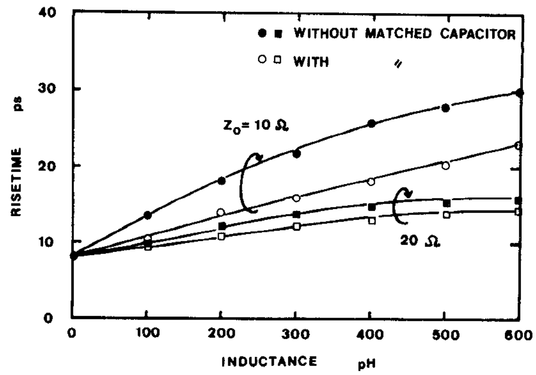

Fig. 3. Relationship between signal rise time and summed inductance at each connector.

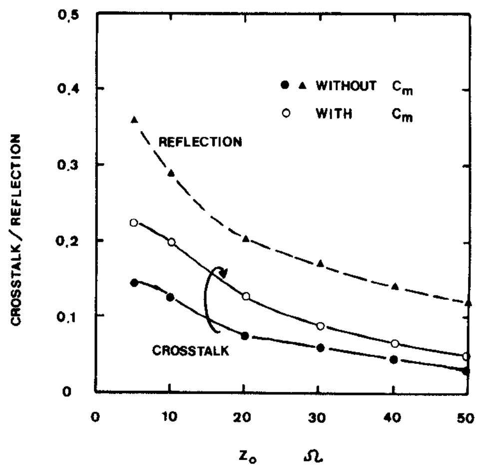

Fig. 4. The current reflection amplitude and absolute value of the crosstalk versus the characteristic impedance value, where L_c is 100 pH and M_c is 40 pH.

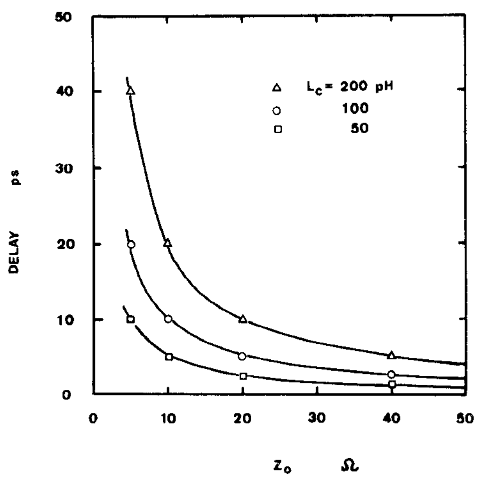

Fig. 5. Relationship between propagation delay at inductive connectors with matched capacitors and characteristic impedance.

in improvement of the degradation with and/or without matching capacitors becomes smaller for a higher characteristic impedance of $Z_0 = 20\ \Omega$.

Second, signal reflection and crosstalk values for $L_c = 100$ pH and $M_c = 40$ pH at each connector are shown for various impedance values in Fig. 4. The reflection coefficient becomes smaller for larger characteristic impedance. Crosstalk values decreased to 1/3 for $Z_0 = 40\ \Omega$ compared with $Z_0 = 10\ \Omega$. An improvement

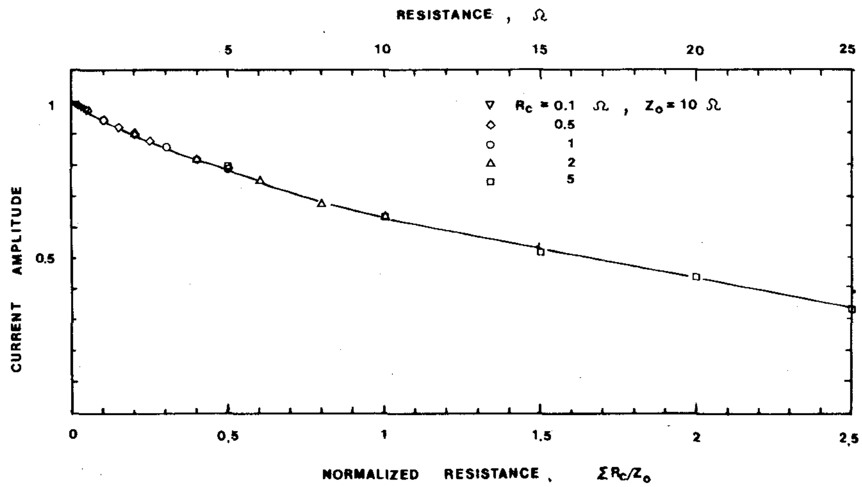

Fig. 6. Relationship between relative current amplitude and summed resistance values as normalized by the characteristic impedance $\Sigma R_c/Z_0$.

in crosstalk is not so large compared with the case of degradation in rise time, because a higher impedance gives an improvement in merits of degradation in rise time. Also, crosstalk becomes larger for the matched transmission line compared with the case of the unmatched line, and, for increasing Z_0, the difference becomes small. Delays at the inductive connectors are shown in Fig. 5. The relationship between calculated propagation delay τ_π and the characteristic impedance Z_0 are shown for various lumped inductances with matched capacitors. It is found that as the characteristic impedance becomes smaller, the propagation delay becomes larger for the same L_c value. For example, the improvement effect for the $Z_0 = 40\ \Omega$ is 1/4 the delay decrease compared with the case of $Z_0 = 10\ \Omega$.

Lastly, the relationship between the transmitted relative current amplitude after the first upward change at each discontinuity, and the summed interconnection resistance values is shown in Fig. 6. Here, if the interconnection resistance values are small enough to be ignored in comparison with the transmission-line characteristic impedance Z_0 (such as at $R_c = 0.1\ \Omega$ is $R_c/Z_0 = 0.01$ for $Z_0 = 10\ \Omega$), amplitude decay due to the interconnection resistances is sufficiently small. Accordingly, for this case, the higher Z_0 is useful. As a typical value for the case of $\Sigma R_c = 1\ \Omega$ for $Z_0 = 10\ \Omega$, the relative current amplitude becomes 0.95. On the other hand, typical resistance values for the chip connector, fillets, and microconnectors have been reported as 80 $\mu\Omega$, 100 $\mu\Omega$, and 1 mΩ, respectively. Accordingly, in comparison with current amplitude distortion caused by slightly unmatched termination resistor values after fabrication [5], these amplitude decays due to interconnection resistance values may be ignored over the range of above $Z_0 = 10\ \Omega$.

III. Discussion

The choice of a higher characteristic impedance on package parts makes electrical distortion at the inductive and resistive connectors smaller. Both of the driver and the receiver circuits work as buffer gates. Accordingly, the present choice of the impedance value of 10–12 Ω on the device chip is available, and so a mixed Z_0 system on the device chips and package parts can be practical. Moreover, the choice of a higher Z_0 on the device chip can make the crossing delay, the rise time, and the current reflection noise small, which are caused by the inductive gate control line at the terminated transmission-line logic [14], such as the capacitively matched three-junction SQUID OR gate [15], and can omit those matched capacitors. Here, the upper limit of the characteristic impedance value will be discussed.

First, consider the cutoff frequency determined by matched inductive connectors. The cutoff frequency (3-dB down) f_c is given by $1/\pi\sqrt{2L_cC_m} = Z_0/\pi L_c$. Accordingly, increasing the characteristic impedance means increasing the cutoff frequency for the same interconnective inductance. For example, for the case of $L_c = 100$ pH, the cutoff frequency is 32 GHz for $Z_0 = 10\ \Omega$, while its value is 122 GHz for $Z_0 = 40\ \Omega$. Therefore, it is found that the higher impedance choice makes the electrical distortion smaller. Moreover, it is enough to use smaller matching capacitors for the higher characteristic impedance if the interconnection inductance is the same value.

In order to reduce amplitude distortion of transmitting ultrafast signals in superconducting systems (in particular, Josephson packaging), it is most important not only to reduce the interconnection inductance values but also to realize a uniform superconducting transmission line with higher Z_0 and well-matched termination resistors. On the other hand, in order to realize higher impedance superconducting transmission lines, the linewidth must be small. For example, the characteristic impedance of thin lead-alloy superconducting stripline over a Nb groundplane with 2-μm linewidth and a SiO insulation layer thickness of 1 μm is 40 Ω. However, if the insulation layer is made thicker to realize a higher characteristic impedance, the fringing factor abruptly becomes larger [16]. Therefore, superconducting striplines with $Z_0 = 40$–$50\ \Omega$ and high-aspect ratios are actual fabrication limits. The coupling between two adjacent superconducting transmission lines has been evaluated in detail by W. H. Chang. The coupling coefficient, defined as the ratio of the mutual inductance to the self-inductance, is small, about 0.6 percent for the case when the linewidth is 2.5 μm and the spacing between the lines is 3 μm on 0.2-μm oxide ($\sim 12\ \Omega$) [17]. It increases to about 3.75 percent for the case of 1-μm oxide [17]. The larger coupling coefficient of the higher Z_0 with thick insulation will give the upper limit of the neighboring line length and the line density according to the noise margin packaging design.

Another limiting factor is the sensitivity of the Josephson receiver. The higher characteristic impedance decreases the output transmitted amplitude of the Josephson drivers, so the highly sensitive receiver is needed. The relationship between the signal steering current ΔI in the transmission line and the characteristic impedance is shown in Fig. 7. Currently, the minimum control

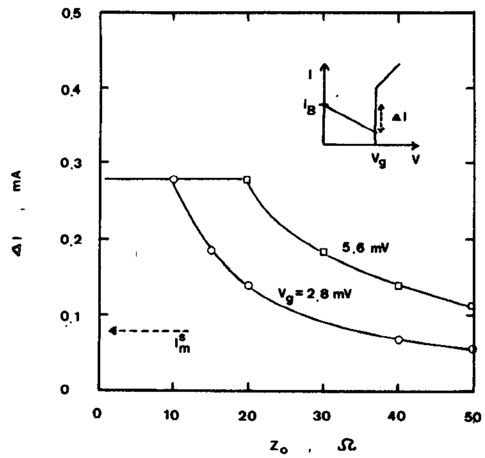

Fig. 7. Relationship between output currents ΔI and the characteristic impedance for Josephson packaging, where bias current I_B is 0.28 mA.

current I_m^s is about 0.08 mA for the case of a Josephson CIL receiver [4], considering the existence of thermal noise. When a higher characteristic impedance is used, the output voltage of the lead-alloy Josephson driver, with gap voltage $V_g = 2.8$ mV, is not sufficient, as shown in Fig. 7. It is necessary to use Josephson drivers which consist of higher gap energy superconductors such as NbN, or $2V_g$ operation drivers. For those drivers with high drivability, the limitation of the receiver sensitivity is not a serious problem. In particular, the device chips and packaging parts, which consist of the Nb–NbN/Nb_2O_5/NbN–Nb junction systems with $V_g = 4.2$ mV [18] and higher Z_0 Nb/NbN superconducting striplines with Nb ground planes, are preferable and can be practical in the near future from the viewpoints of low-noise electrical properties and reliable mechanical construction.

In order to realize large-scale superconducting systems, devices with high drivability, highly sensitive receivers, and high-impedance superconducting transmission lines are needed. When a higher impedance of $Z_0 = 40$–$50\ \Omega$ is used in superconducting packaging, the matching capacitor does not play as important a role and should be omitted from the standpoint of decreasing crosstalk.

IV. Conclusion

The characteristic impedance influences of superconducting packaging systems (in particular, Josephson packaging) on fast switching signal propagation characteristics such as degraded switching time, amplitude distortions and crosstalk, signal propagation delay, and amplitude decay at the inductive and resistive connectors with matched capacitors were quantitatively evaluated for the first time by using the ASTAP computer simulation. The present choice of the characteristic impedance $Z_0 = 10$–$12\ \Omega$ for a superconducting stripline is not adequate. The higher impedance of $Z_0 = 40$–$50\ \Omega$ is useful from the standpoint of noise margin. A higher impedance choice makes ground connectors of the various connectors decrease, which is very useful for the large-scale package system.

In summary, in order to reduce amplitude distortions of transmitted ultrafast sig als in superconducting technology, it is important not only to ɔduce the interconnection inductance values, but also to realize niform transmission superconducting lines with a higher characteristic impedance of $Z_0 = 40$–$50\ \Omega$, a highly sensitive superconductive receiver, and a superconducting driver with large drivability.

Acknowledgment

The authors would like to thank K. Aoki, Y. Tazoh, and K. Satoh for their valuable discussions in the initial stages of this study. They also wish to extend their gratitude to Dr. J. Matisoo for his valuable comments.

References

[1] R. L. Kautz, "Picosecond pulses on superconducting striplines," *J. Appl. Phys.*, vol. 49, pp. 308–314, Jan. 1978.
[2] W. Anacker, "Computing at 4 degrees Kelvin," *IEEE Spectrum*, pp 26–37, May 1979.
[3] H. C. Jones and D. J. Herrell, "The characteristics of chip-to-chip signal propagation in a package suitable for superconducting circuits," *IBM J. Res. Develop.*, vol 24, pp 172–177, Mar. 1980.
[4] M. Klein, "Chip-to-chip driver and receiver circuits for a Josephson computer," *IEEE J. Solid-State Circuits*, vol. SC-17, pp. 739–742, Aug. 1982.
[5] J. Temmyo and H. Yoshikiyo, "Numerical evaluation of lumped inductance influences of superconducting circuits interconnections on ultrafast switching signal propagation characteristics," *IEEE Trans. Microwave Theory Tech.*, vol. MTT-30, pp. 27–34, Jan. 1982.
[6] C J Anderson, M. Klein, and M. B. Ketchen, "Transmission of high speed electrical signals in a Josephson package," *IEEE Trans. Magn.*, vol. MAG-19, pp. 1182–1185, May 1983.
[7] E. E. Davidson, "Electrical design of a high speed computer package," *IBM J. Res. Develop.*, vol. 26, pp. 349–361, May 1982.
[8] IBM Advanced Statistical Analysis Program, IBM Publ. No. SH20-1118, available through IBM branch office.
[9] C. Y. Ting, K. B. Grebe, and D. P. Waldman, "Controlled collapse reflow for Josephson chip bonding," in *Proc. Electrochemical Soc. Conf.*, May 1980, pp. 210–212.
[10] J. Temmyo, K. Aoki, H. Yoshikiyo, S. Tsurumi, and Y. Takeuchi," Solder bump height dependence of Josephson chip-to-card interconnection inductance using flip chip bonding technique," *J. Appl. Phys.*, vol. 54, pp. 5282–5286, Sept. 1983.
[11] K. R. Grebe, C. Y. Ting, and D. P. Waldman, "Orthogonal solder interconnections for Josephson packaging," in *Proc. Electrochemical Soc. Conf.*, May 1980, pp. 213–215.
[12] S. K. Lahiri, P. Geldermans, G. Kolb, J. Sokolowski, and M. J. Palmer, "Pluggable connectors for Josephson device packaging," in *Proc. Electrochemical Soc. Conf.*, May 1980, pp. 216–217.
[13] M. B. Ketchen *et al.*, "A Josephson system level experiment," *IEEE Electron Device Lett.*, vol. EDL-2, pp. 262–265, Oct. 1981.
[14] H. H. Zappe, "Josephson quantum interference computer devices," *IEEE Trans Magn.*, vol. MAG-13, pp. 41–47, Jan 1977.
[15] T. R. Gheewala, "A 30 ps Josephson current injection logic (CIL)," *IEEE Solid-State Circuits*, vol. SC-14, pp. 787–793, Oct. 1979.
[16] W. H. Chang, "The inductance of superconducting strip transmission line," *J. Appl. Phys.*, vol. 50, pp. 8129–8134, Dec. 1979
[17] W. H. Chang, "Measurement and calculation of Josephson junction device inductances," *J. Appl. Phys.*, vol. 52, pp. 1417–1426, Mar. 1981.
[18] A. Shoji, S. Kosaka, F. Shinoki, M. Aoyagi, and H. Hayakawa, "All refractory Josephson tunnel junctions fabricated by reactive ion etching," *IEEE Trans. Magn.*, vol. MAG-19, pp. 827–830, May 1983.

Calculation of High-Resolution SAR Distributions in Biological Bodies Using the FFT Algorithm and Conjugate Gradient Method

DAVID T. BORUP AND OM P. GANDHI, FELLOW, IEEE

Abstract —**A new method for the calculation of absorption in inhomogeneous, lossy dielectrics is presented. In this method, the convolutional nature of the electric-field integral equation is exploited by use of the FFT algorithms and the conjugate gradient method (CGM). The method is illustrated by solving for the SAR distribution for an anatomical cross section through the human eyes at 1 GHz.**

Manuscript received June 20, 1984; revised January 4, 1985. This work was supported in part by the NIEHS under Grant ES 02304.

The authors are with the Department of Electrical Engineering, University of Utah, Salt Lake City, Utah 84112.

0018-9480/85/0500-0417$01.00 ©1985 IEEE